

Magnetocaloric effect and magnetostructural coupling in $\text{Mn}_{0.92}\text{Fe}_{0.08}\text{CoGe}$ compound

J. L. Wang, P. Shamba, W. D. Hutchison, Q. F. Gu, M. F. Md Din, Q. Y. Ren, Z. X. Cheng, S. J. Kennedy, S. J. Campbell, and S. X. Dou

Citation: *Journal of Applied Physics* **117**, 17D103 (2015); doi: 10.1063/1.4906437

View online: <http://dx.doi.org/10.1063/1.4906437>

View Table of Contents: <http://scitation.aip.org/content/aip/journal/jap/117/17?ver=pdfcov>

Published by the AIP Publishing

Articles you may be interested in

[Phase diagram and magnetocaloric effects in \$\text{Ni}_{1-x}\text{Cr}_x\text{MnGe}_{1.05}\$](#)

J. Appl. Phys. **117**, 17A711 (2015); 10.1063/1.4907765

[The magnetic phase transition in \$\text{Mn}_{1.1}\text{Fe}_{0.9}\text{P}_{1-x}\text{Ge}_x\$ magnetocaloric alloys](#)

J. Appl. Phys. **117**, 063909 (2015); 10.1063/1.4906568

[On the crystal structure and magnetic properties of the \$\text{Mn}_{0.94}\text{Ti}_{0.06}\text{CoGe}\$ alloy](#)

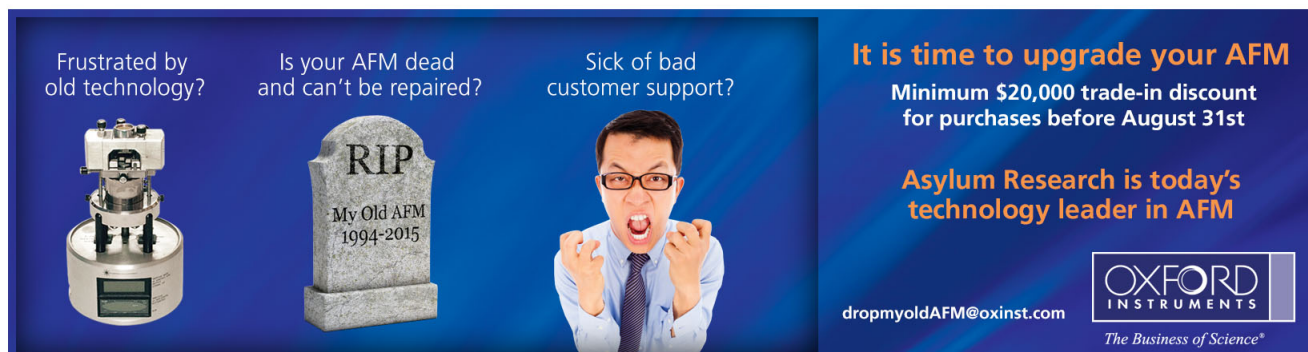
J. Appl. Phys. **113**, 17A941 (2013); 10.1063/1.4801523

[Giant magnetocaloric effects near room temperature in \$\text{Mn}_{1-x}\text{Cu}_x\text{CoGe}\$](#)

Appl. Phys. Lett. **101**, 242405 (2012); 10.1063/1.4770379

[Tunable thermal hysteresis in \$\text{MnFe}\(\text{P},\text{Ge}\)\$ compounds](#)

Appl. Phys. Lett. **94**, 102513 (2009); 10.1063/1.3095597



Frustrated by old technology? Is your AFM dead and can't be repaired? Sick of bad customer support?

It is time to upgrade your AFM
Minimum \$20,000 trade-in discount for purchases before August 31st

Asylum Research is today's technology leader in AFM

dropmyoldAFM@oxinst.com

OXFORD INSTRUMENTS
The Business of Science®

The advertisement features three images: an old AFM, a tombstone for 'My Old AFM 1994-2015', and a man shouting in frustration.

Magnetocaloric effect and magnetostructural coupling in $\text{Mn}_{0.92}\text{Fe}_{0.08}\text{CoGe}$ compound

J. L. Wang,^{1,2,a)} P. Shamba,¹ W. D. Hutchison,³ Q. F. Gu,⁴ M. F. Md Din,¹ Q. Y. Ren,³ Z. X. Cheng,¹ S. J. Kennedy,² S. J. Campbell,³ and S. X. Dou¹

¹*Institute for Superconductivity and Electronic Materials, University of Wollongong, Wollongong, NSW 2522, Australia*

²*Bragg Institute, Australian Nuclear Science and Technology Organization, Lucas Heights, NSW 2234, Australia*

³*School of Physical, Environmental and Mathematical Sciences, The University of New South Wales, Canberra, ACT 2600, Australia*

⁴*Australian Synchrotron, 800 Blackburn Rd, Clayton 3168, Australia*

(Presented 5 November 2014; received 22 September 2014; accepted 7 October 2014; published online 23 January 2015)

The structural properties of $\text{Mn}_{0.92}\text{Fe}_{0.08}\text{CoGe}$ have been investigated in detail using synchrotron x-ray diffraction in zero and applied pressure ($p=0\text{--}10\text{ GPa}$). A ferromagnetic transition occurs around $T_C=300\text{ K}$ and a large magnetic-entropy change $-\Delta S_M=17.3\text{ J/kg K}$ detected at T_C for a field change of $\Delta B=5\text{ T}$. The field dependence of $-\Delta S_M^{\text{max}}$ can be expressed as $-\Delta S_M^{\text{max}} \propto B$. At ambient temperature and pressure, $\text{Mn}_{0.92}\text{Fe}_{0.08}\text{CoGe}$ exhibits a co-existence of the orthorhombic TiNiSi -type structure (space group Pnma) and hexagonal Ni_2In -type structure (space group P63/mmc). Application of external pressure drives a structure change from the orthorhombic TiNiSi -type structure to the hexagonal Ni_2In -type structure. A large anomaly in heat capacity around T_C is detected and the Debye temperature $\theta_D (=319(\pm 10)\text{ K})$ has been derived from analyses of the low temperature heat capacity, $T \lesssim 10\text{ K}$. © 2015 AIP Publishing LLC.

[<http://dx.doi.org/10.1063/1.4906437>]

Magnetocaloric materials have attracted significant interests over the past two decades due to their possible applications as high efficiency, environmentally friendly heat pumps and refrigerators. This follows the discoveries reported by Pecharsky and Gschneidner in 1997 related to magnetic entropy changes at ferromagnetic transitions in the $\text{Gd}_5\text{Si}_{4-x}\text{Ge}_x$ series.¹ More recently, compounds containing manganese such as $\text{MnFeP}_{0.45}\text{As}_{0.55}$,² $\text{MnAs}_{1-x}\text{Sb}_x$,³ Ni-Mn-Sn-based alloys,⁴ Ni-Mn-Ga,⁵ RMn_2X_2 -based,⁶ and $\text{MnCoGe}/\text{MnNiGe}$ -based compounds⁷ have attracted significant attention due to their interesting magnetic properties and large entropy changes. These large entropy changes and related magnetocaloric effects result from the high sensitivity of Mn magnetic states to variations in the chemical environment.

Stoichiometric MnCoGe has an orthorhombic TiNiSi -type structure (space group Pnma) at low temperatures (below $\sim 650\text{ K}$) and exhibits a martensitic structural transformation⁸ from the low-temperature orthorhombic TiNiSi -type structure to a high-temperature hexagonal Ni_2In -type structure (space group P63/mmc) around $T_{\text{str}}=650\text{ K}$. The MnCoGe compounds in both structural states are ferromagnets but their magnetizations and Curie temperatures (T_C) differ considerably ($T_C=345\text{ K}$ for the orthorhombic structure, $T_C=275\text{ K}$ for the hexagonal structure). Importantly, the value of T_{str} depends strongly on several factors including: external pressure,⁸ the vacancies in the Co and Mn sites, as well as variation in chemical environment due to element

substitution on Mn, Co, or Ge sites.^{9–17} Recently, MnCoGe -based compounds have attracted significant attention;^{9–17} this is due mainly to the strong coupling between magnetism and structure in these materials. This coupling in turn can lead to MnCoGe -based materials, which exhibit large entropy changes and associated magnetocaloric effects, thereby offering scope for magnetic refrigeration around room temperature. In order to achieve coincidence of magnetic and structural transitions which differ by around 300 K in the parent MnCoGe compound, several approaches to modify the Mn environments have been adopted.^{9–17} Several studies concerning substitution of other elements for Mn, Co, or Ge have been reported in order to shift and thereby control the transition temperatures T_{str} and T_C .^{9–14} The general aim of such studies is to cause the magnetic and structural transitions to coincide or overlap closely and thereby capitalise on both the magnetic and structural entropies at the resultant magnetostructural transition.^{10–14}

In this work, we report the structural and magnetic properties of $\text{Mn}_{0.92}\text{Fe}_{0.08}\text{CoGe}$ compound as determined by high resolution, high intensity synchrotron x-ray diffraction studies and detailed magnetic measurements. We also report the influence of external pressure ($0\text{--}10\text{ GPa}$) on the structural properties of $\text{Mn}_{0.92}\text{Fe}_{0.08}\text{CoGe}$ as determined by high resolution synchrotron studies.

$\text{Mn}_{0.92}\text{Fe}_{0.08}\text{CoGe}$ was prepared by argon arc melting appropriate amounts of high purity elements on a water-cooled Cu hearth. Around 3% excess Mn was added to compensate for loss during melting. The sample was re-melted five times to ensure good homogeneity and annealed at $850\text{ }^\circ\text{C}$ for 1

^{a)}Author to whom correspondence should be addressed. Electronic mail: jianli@uow.edu.au.

week in an evacuated quartz tube then quenched into water. X-ray diffraction (Cu K_{α}) at room temperature confirmed that both the orthorhombic TiNiSi-type structure (space group Pnma) and hexagonal Ni_2In -type structure (space group P63/mmc) are present in the sample with no discernible impurity phases. The magnetic measurements were carried out using a Physical Property Measurement System over the temperature range of 5–340 K and at magnetic fields in the range of 0–8 T. The high pressure diffraction studies at room temperature were undertaken using the Powder Diffraction (PD) beamline at the Australian Synchrotron facility in the pressure range from ambient to 10 GPa using a diamond anvil cell.

Figure 1(a) shows a series of diffraction patterns for the $Mn_{0.92}Fe_{0.08}CoGe$ compound collected at different pressures. At ambient pressure, it can be seen that there are mixtures of

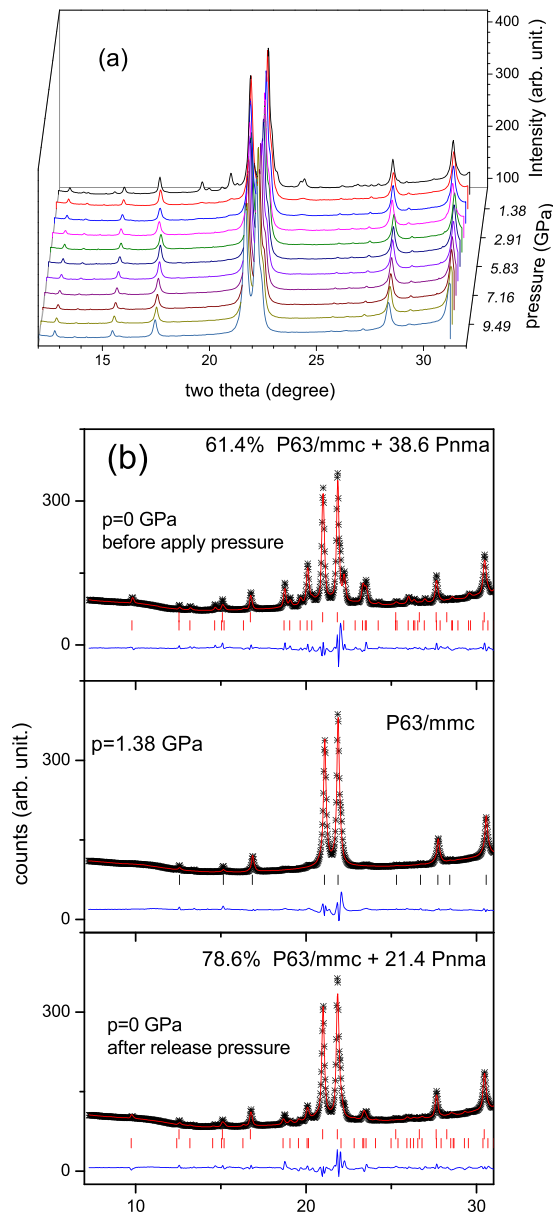


FIG. 1. (a) Synchrotron x-ray diffraction patterns of $Mn_{0.92}Fe_{0.08}CoGe$ at room temperature and at various external pressures from 0 GPa to 9.94 GPa; (b) Rietveld refinements of x-ray patterns at $p=0$ GPa (before applying pressure), $p=1.38$ GPa, and $p=0$ GPa (after release of pressure).

the orthorhombic TiNiSi-type structure ($\sim 61.4\%$) and the hexagonal Ni_2In -type structure ($\sim 38.6\%$). The lattice parameters for the orthorhombic structure have been derived to be $a=5.910(6)$ Å, $b=3.832(5)$ Å, $c=7.083(6)$ Å, and $V=160.4(3)$ Å³, while $a=4.089(4)$ Å, $c=5.322(3)$ Å, and $V=77.0(1)$ Å³ for the hexagonal phase. On applying hydrostatic pressure above $p=1.38$ GPa, the compound was found to exhibit only the hexagonal Ni_2In -type structure. This finding indicates that application of external pressure results in a phase transition from the orthorhombic TiNiSi-type structure of $Mn_{0.92}Fe_{0.08}CoGe$ into the hexagonal Ni_2In -type structure. In other words, the external pressure is found to shift the structural transition temperature from above room temperature down to below room temperature. Rietveld refinements results of $Mn_{0.92}Fe_{0.08}CoGe$ (FULLPROF software) at selected pressures are shown in Figure 1(b). Before applying pressure, there is around $\sim 61\%$ of the orthorhombic phase and $\sim 39\%$ of the hexagonal at room temperature. When the applied pressure is greater than $p \sim 1.38$ GPa, the structure of the entire sample changes to the hexagonal structure. However, it should be noted that on release of the pressure, the overall sample structures revert to a mixture of both orthorhombic and hexagonal of phase fractions $\sim 78.6\%$ orthorhombic and 21.4% hexagonal. This behaviour demonstrates that the structural modification by external pressure is partially reversible. The outcomes of our experiment indicate that external pressure drives the structure transition temperatures of $Mn_{0.92}Fe_{0.08}CoGe$ down to below room temperature. This agrees well with the conclusion obtained for the parent MnCoGe compound by Niziol *et al.*,⁸ who reported that external pressure can lead to a significant decrease in the transition temperature under hydrostatic pressure up to 1.3 GPa.

The pressure dependences of the lattice parameters derived from the refinements are shown in Figure 2. It can be seen from the variation of the c/a ratio with pressure (inset to Figure 2(b)) that the contraction of the unit cell with pressure is anisotropic. It is well accepted that the lattice response to pressure can be described by the Murnaghan equation as follows:

$$P(V) = \frac{B_0}{B_0'} \left(\left(\frac{V_0}{V} \right)^{B_0'} - 1 \right) \quad (1)$$

or equivalently

$$V(P) = V_0 \left(1 + B_0' \frac{P}{B_0} \right)^{-1/B_0'}, \quad (2)$$

where V_0 , B_0 , and B_0' are the volume, bulk modulus, and its first derivative at ambient pressure, respectively.

The experimental data have been fitted with 3rd order of Murnaghan equation leading to the fitted results shown by the full line in Figure 2(b). The values of B_0 and B_0' for $Mn_{0.92}Fe_{0.08}CoGe$ have been derived to be 112.2 GPa and 7.2, respectively. By comparison, the values of B_0 for $TbNi_2Mn$ and $TbNi_2$ (Ref. 18) are found to be 128 GPa and 103 GPa, respectively, while B_0 is only 68 GPa and 20 GPa for $Pr_{0.5}Y_{0.5}Mn_2Ge_2$ (Ref. 6) and $TbMn_2$,¹⁹ respectively.

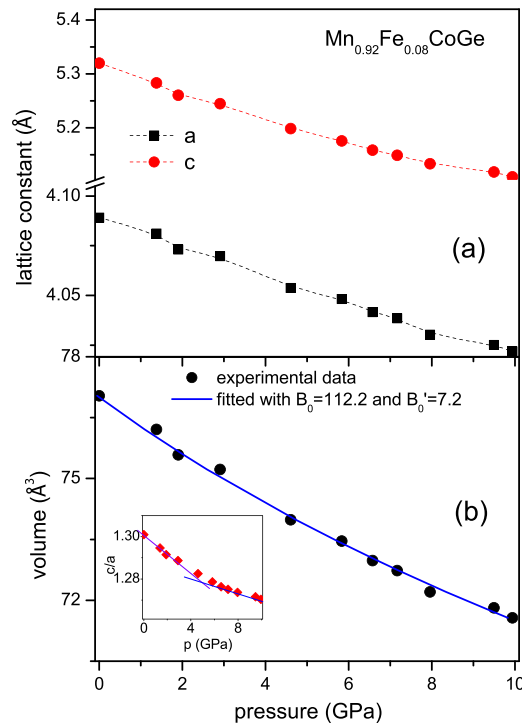


FIG. 2. (a) Lattice parameters *a*, *c* and (b) unit cell volume as a function of external pressure for Mn_{0.92}Fe_{0.08}CoGe. The full line in Figure 2(b) represents a fit to the Murnaghan equation as described in the text. The inset shows the change in *c/a* ratio with pressure.

The temperature dependence of the DC magnetization (see Figure 3) reveals only one magnetic phase transition in Mn_{0.92}Fe_{0.08}CoGe with $T_C = 300(\pm 5)$ K; this behaviour agrees well with the differential scanning calorimetry (DSC) measurements shown as the inset of Figure 3. This behaviour of a unique transition temperature in the magnetisation and DSC results indicates that the structure and magnetic transitions coincide in this compound. The magnetization of Mn_{0.92}Fe_{0.08}CoGe as measured as a function of field over the temperature region 120 K to 350 K with 5 K steps is shown in Figure 4(a). The related Arrott plots of M^2 versus B/M at selected temperatures are drawn in Figure 4(b) with the positive slopes of the Arrott plots around T_C indicating that the magnetic transition around T_C

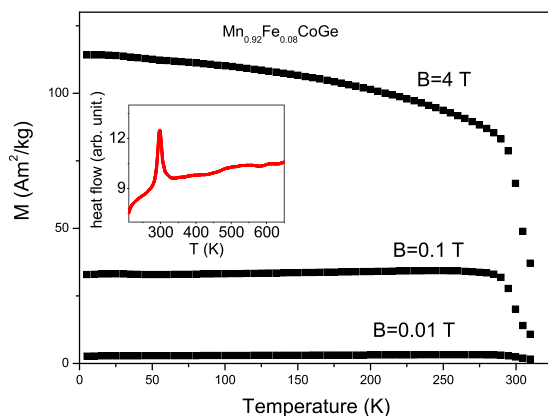


FIG. 3. The temperature dependence of the magnetization of Mn_{0.92}Fe_{0.08}CoGe under various fields. The inset shows the DSC curve obtained over the temperature range of ~230 K to 650 K.

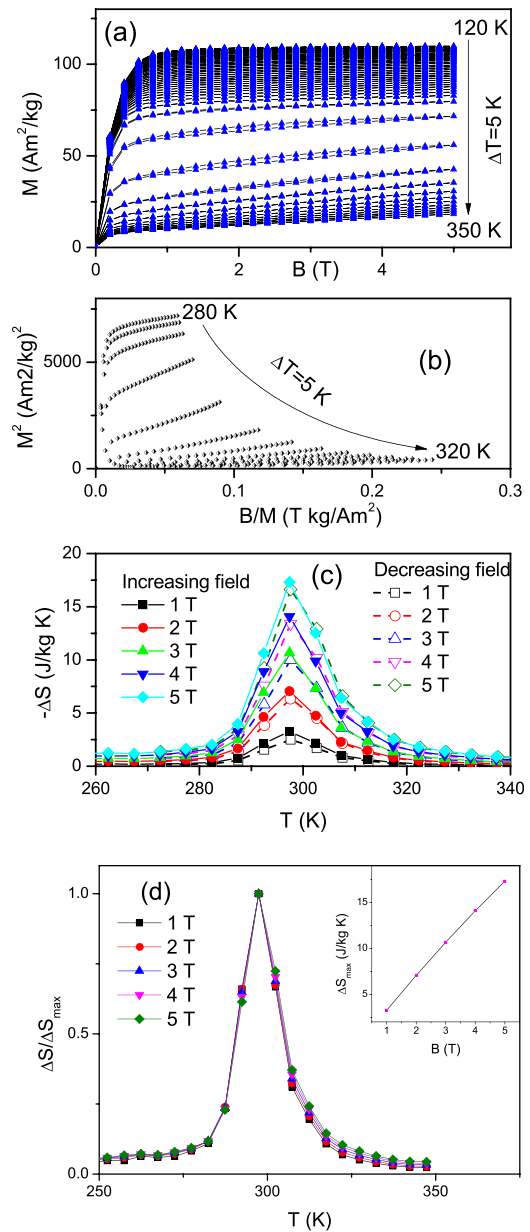


FIG. 4. (a) The variation in magnetization with applied magnetic field $B = 0-5$ T at the temperatures indicated for Mn_{0.92}Fe_{0.08}CoGe. (b) The Arrott-plots of M^2 versus B/M at the temperatures indicated. (c) Temperature dependence of the isothermal magnetic entropy change $-\Delta S_M(T, B)$ calculated from the magnetization isotherms. (d) The normalized entropy change $\Delta S_M / \Delta S_M^{\text{peak}}$ for Mn_{0.92}Fe_{0.08}CoGe as a function of temperature. The inset to Figure 4(d) shows a graph of maximum values of the entropy change $-\Delta S_M^{\text{max}}$ with magnetic field.

is second order. The isothermal entropy change $-\Delta S_M$ corresponding to magnetic field change ΔB (starting from zero field) can be conveniently derived from the magnetization data using the Maxwell relation [e.g., Refs. 2–6]

$$\Delta S_M(T, B) = \int_0^B \left(\frac{\partial M(T, B)}{\partial T} \right)_B dB.$$

The magnetocaloric entropy change determined in this way is shown in Figure 4(c) with the curves for decreasing field and increasing field found to be essentially identical. The maximum entropy changes for $\Delta B = 1$ T and $\Delta B = 5$ T are

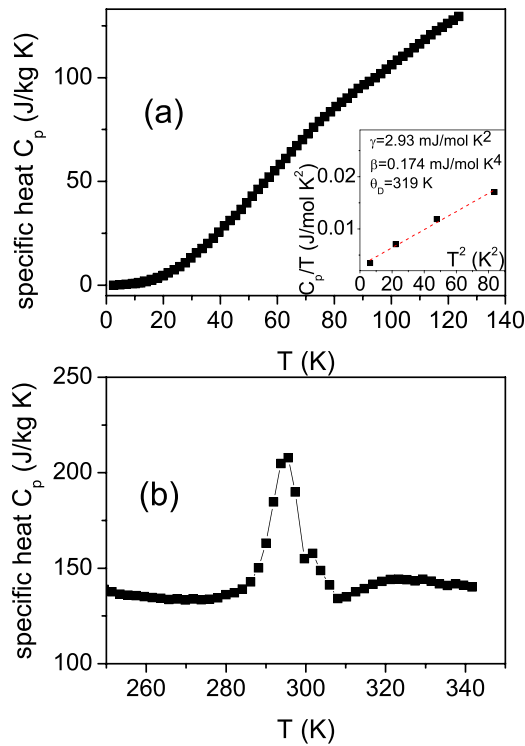


FIG. 5. Heat capacity C_p for the $\text{Mn}_{0.92}\text{Fe}_{0.08}\text{CoGe}$ compound: (a) in the lower temperature regime from 2 K to 120 K and (b) the higher temperature regime from 250 K to 340 K. The inset of Figure 5(a) shows the C_p/T versus T^2 plot from 2 K to 10 K with the linearly fitted curve shown as a dashed line.

3.2/kg K and 17.2 J/kg K, respectively. The latter entropy value for $\text{Mn}_{0.92}\text{Fe}_{0.08}\text{CoGe}$ around $T_c \sim 300$ K is close to the values obtained in $\text{Mn}_{0.88}\text{Fe}_{0.12}\text{CoGe}$ (16.5 J/kg K around 242 K (Ref. 16)) and in $\text{Gd}_5\text{Si}_2\text{Ge}_2$ (18 J/kg K around 276 K (Ref. 1)) under a field change of $\Delta B = 5$ T. The entropy change in the present $\text{Mn}_{0.92}\text{Fe}_{0.08}\text{CoGe}$ sample is larger than values reported for Fe substitution for Mn in MnCoGe such as 10.6 J/kg K in $\text{Mn}_{0.97}\text{Fe}_{0.03}\text{CoGe}$ alloys,¹⁵ 16.5 J/kg K in $\text{Mn}_{0.88}\text{Fe}_{0.12}\text{CoGe}$ and 13 J/kg K in $\text{Mn}_{0.87}\text{Fe}_{0.13}\text{CoGe}$.¹⁶ This enhanced value for the entropy change in the present sample is likely to be due to coincidence of the structural and magnetic phase transitions where both structural entropy and magnetic entropy are found to contribute significantly to the total entropy change around T_c . Moreover, it was found that the maximum values of the entropy change $-\Delta S_M^{\max}$ vary almost linearly with magnetic field (inset to Figure 4(d)), indicating that the proportional relationship $-\Delta S_M^{\max} \propto B$ applies at this transition. As described in the literature, the relationship of the lattice parameters between orthorhombic and hexagonal structures can be represented as: $a_{\text{ortho}} = c_{\text{hex}}$, $b_{\text{ortho}} = a_{\text{hex}}$, $c_{\text{ortho}} = \sqrt{3}a_{\text{hex}}$, and $V_{\text{ortho}} = 2V_{\text{hex}}$.

Using the room temperature lattice parameters, we can see that the unit cell of the orthorhombic structure contracts around 4% on changing to the hexagonal structure, thereby introducing additional structural entropy.²⁰ Figure 4(d) shows a graph of the normalized entropy change $\Delta S_M(T)/\Delta S_M^{\max}$ for $\text{Mn}_{0.92}\text{Fe}_{0.08}\text{CoGe}$ versus temperature. It can be seen that when normalised in this way, the field dependent entropy curves effectively collapse into a single curve.

The temperature dependence of the heat capacity measurements $C_p(T)$ for $\text{Mn}_{0.92}\text{Fe}_{0.08}\text{CoGe}$ at lower (2 K–120 K) and higher temperature (250 K–340 K) regions is shown in Figures 5(a) and 5(b), respectively. The pronounced anomaly observed around T_c originates from coincidence of the structural and magnetic phase transitions. It is well accepted that the total heat capacity $C_p(T)$ includes three contributions from phonon $C_{\text{ph}}(T)$, electrons $C_{\text{el}}(T)$, and magnons $C_{\text{m}}(T)$, respectively. At low temperatures, the heat capacity can be described as $C(T) = \gamma T + \beta T^3$, where γT represents the electronic contribution and βT^3 comes from the phonon contribution. By fitting the graph of C_p/T versus T^2 (see inset of Figure 5(a)), the values of $\gamma = 2.93$ mJ/mol K^2 and $\beta = 0.174$ mJ/mol K^4 have been derived. The Debye temperature θ_D can be obtained from the β value to be $\theta_D = 319(\pm 10)$ K, which is very close to the values reported for $\text{Mn}_{0.8}\text{Fe}_{0.2}\text{CoGe}$ ($\theta_D = 306$ K)¹⁷ and $\text{CoMnGe}_{0.945}\text{Ga}_{0.055}$ ($\theta_D = 337$ K).²¹

The structural and magnetic properties of $\text{Mn}_{0.92}\text{Fe}_{0.08}\text{CoGe}$ have been investigated over the temperature range of 5–650 K. At ambient temperature and pressure, $\text{Mn}_{0.92}\text{Fe}_{0.08}\text{CoGe}$ exhibits co-existence of the orthorhombic TiNiSi -type structure (space group Pnma) and hexagonal Ni_2In -type structure (space group P63/mmc). Application of external pressure ($p = 1.38$ GPa) drives a structure change from the orthorhombic TiNiSi -type structure to the hexagonal Ni_2In -type structure. The $\text{Mn}_{0.92}\text{Fe}_{0.08}\text{CoGe}$ compound exhibits a pronounced magnetostructural transition around $T_c \sim 300$ K. A large magnetic-entropy change of $-\Delta S_M = 17.3$ J/kg K at T_c for a field change of $\Delta B = 5$ T has been determined for the $\text{Mn}_{0.92}\text{Fe}_{0.08}\text{CoGe}$ compound. The field dependence of $-\Delta S_M^{\max}$ around T_c can be expressed as $-\Delta S_M^{\max} \propto B$.

This work was supported in part by Discovery Grant DP110102386 from the Australian Research Council. Part of the experiment was conducted at the Powder Diffraction beamline of the Australian Synchrotron.

- ¹V. K. Pecharsky *et al.*, *Phys. Rev. Lett.* **78**, 4494 (1997).
- ²O. Tegus *et al.*, *Nature (London)* **415**, 150 (2002).
- ³H. Wada *et al.*, *Appl. Phys. Lett.* **79**, 3302 (2001).
- ⁴T. Krenke *et al.*, *Nature Mater.* **4**, 450 (2005).
- ⁵A. A. Cherechukin *et al.*, *Phys. Lett. A* **326**, 146 (2004).
- ⁶J. L. Wang *et al.*, *Phys. Rev. Lett.* **110**, 217211 (2013).
- ⁷E. K. Liu *et al.*, *Nat. Commun.* **3**, 873 (2012); E. K. Liu *et al.*, *Appl. Phys. Lett.* **102**, 122405 (2013).
- ⁸S. Niziol *et al.*, *J. Magn. Magn. Mater.* **38**, 205 (1983).
- ⁹J. C. Debnath *et al.*, *J. Appl. Phys.* **113**, 093902 (2013).
- ¹⁰N. T. Trung *et al.*, *Appl. Phys. Lett.* **96**, 162507 (2010).
- ¹¹L. Caron *et al.*, *Phys. Rev. B* **84**, 020414(R) (2011).
- ¹²T. Samanta *et al.*, *Appl. Phys. Lett.* **100**, 052404 (2012).
- ¹³T. Samanta *et al.*, *Appl. Phys. Lett.* **101**, 242405 (2012).
- ¹⁴P. Shamba *et al.*, *J. Phys.: Condens. Matter* **25**, 056001 (2013).
- ¹⁵G. J. Li *et al.*, *J. Magn. Magn. Mater.* **332**, 146 (2013).
- ¹⁶T. Samanta *et al.*, *J. Magn. Magn. Mater.* **330**, 88 (2013).
- ¹⁷T. Samanta *et al.*, *Appl. Phys. Lett.* **103**, 042408 (2013).
- ¹⁸A. Lindbaum *et al.*, *Phys. Rev. B* **65**, 134114 (2002).
- ¹⁹D. D. Jackson *et al.*, *Phys. Rev. B* **75**, 224422 (2007).
- ²⁰K. A. Gschneidner, Jr., *et al.*, *Scr. Mater.* **67**, 572 (2012).
- ²¹I. Dincer *et al.*, *J. Alloys Compd.* **588**, 332 (2014).